J Nanostruct 11(3): 588-600, Summer 2021

RESEARCH PAPER

The Effect of Micro and Nano Size TiC Additions on Some Properties of Copper Fabricated by Powder Metallurgy

Nawal Ali Abd [1] *, Jawdat Ali Yagoob* [2]*, Khalid H. Razeg* [3]*

[1] *Department of Physics , College of Education for Pure Sciences , Tikrit University, Iraq*

[2] *Department of Power Mechanics Techniques , Technical College of Engineering Kirkuk , Northern Technical University, Iraq*

ARTICLE INFO

Article History:
Received 11 March 2021
Accepted 22 May 2021
Published 01 July 2021

Keywords:
Copper-TiC composites
Copper-TiC Properties
Powder metallurgy

ABSTRACT

The goal of this study is to evaluate how micro TiC (1-4.5) wt% and nano TiC (0.25-1) wt% additions effects on the properties of copper base composites made by powder metallurgy. Powder mixes were ball milled for 7 hours at 170 rpm in a 304SS container. Uniaxial pressing at 700 MPa was performed to prepare the samples, and then they are sintered at 850°C for 2 hours in an electric resistance furnace in an argon atmosphere. The results revealed that as the micro and nano TiC content increases, the density of the sintered copper decreases. Generally, the micro size TiC addition tends to increase the porosity of sintered copper samples, while the increase of the porosity was in lower values particularly when the nano TiC addition was greater than 0.25 wt%. The increase in micro TiC addition is reflected in the increase of the micro-hardness of sintered copper, while the best micro-hardness value was measured for the sintered copper sample with the lowest nano TiC addition that was 0.25 wt%. The microstructure of the pure copper sintered compacts and its composites with micro and nano-size TiC additions were analyzed and observed with aid of XRD, optical microscope and FESEM-Mapping, techniques.

How to cite this article
Abd N. A , Yagoob J. A , Razeg K. H. The Effect of Micro and Nano Size TiC Additions on Some Properties of Copper Fabricated by Powder Metallurgy. J Nanostruct, 2021; 11(3):588-600. DOI: 110.22052/JNS.2021.03.016

INTRODUCTION

Metal-matrix composites (MMCs) are currently the subject of considerable study and development around the world; these materials are made by high-pressure infiltration casting and pressure-free metal infiltration. Powder metallurgical procedures, plasma spraying of the matrix material, hot pressing, and self-propagating high-temperature synthesis are some of the other fabrication processes. MMCs can provide greater oxidation resistance at high temperature operating limits, in addition to improved strength, stiffness, and abrasion resistance, and lower density [1-2]. Because ceramic particles have a high hardness and endurance to high temperatures, composites reinforced with particles combine the properties of the metal matrix with the reinforcing properties of ceramics. As a result, composites reinforced with ceramic particles are also used in high-temperature applications. The addition of ceramic particles to the matrix boosts the composite's hardness and abrasion resistance while lowering its electrical conductivity. As a result, Cu -based composites reinforced with ceramic particles are mostly employed in electronics and electro-mechanics for relays, switches, electric motor parts, and resistance welding electrode tips [3-5]. Cu is the material of choice for applications requiring high

* *Corresponding Author Email: khalid.hr.55@tu.Edu.iq*

thermal and electrical conductivity; however, some applications also demand strong hardness and wear resistance in addition to outstanding thermal and electrical conductivity. As a result, extensive research has been conducted to improve copper's mechanical qualities, to achieve grain refinement and dispersion strengthening effects. The reinforcements are usually homogeneously distributed in the Cu matrix in these materials. At room temperature, however, they have a low damage tolerance because the reinforcements prevent the matrix from deforming plastically [6,7]. Because of its high melting point, high Young's modulus, low density, and outstanding conductivity and thermal properties, titanium carbide (TiC), a typical transition metal carbide, is the most extensively utilized phase of particle-reinforced MMCs. It is widely known that the shape of ceramic particles has a significant impact on the performance of ceramic particle-reinforced MMCs, particularly their mechanical performance [8]. TiC has negligible solubility in copper such that the TiC/Cu interface remains free from intermetallic compounds or solid solutions [9]. Due to its high modulus, hardness, melting temperature, and other properties, it has received a lot of attention [10-11]. Due to the high contact angle between the Cu melt and TiC particles, external incorporation of TiC particles into metallic matrices such as Cu causes issues such as dispersoid phase segregation and poor (TiC/matrix) interfacial bonding [12]. TiC ceramics almost always have a unique shape that allows them to be used in a variety of applications. In fact, by manipulating their extrinsic properties, such as sizes and growth morphologies, their successful applications can be greatly expanded [13]. Furthermore, this type of material has proven to be an appropriate candidate for providing knowledge that expands the range of applications, particularly in the aeronautical, automotive, and biomedical fields, where these types of materials are used for applications such as electrical and thermal conduction uses that are mechanical or structural [14]. Because powder metallurgy (PM) techniques are a highly complicated and unpredictable process, determining ideal parameters for the best qualities, such as conductivity and bond strength, which are the most essential output parameters, is quite challenging [15]. It was chosen as the processing method because of the ease with which a hard phase may be incorporated into a metal phase by combining powders. Because of the excellent dispersion of the small reinforcing particles, PM is perfect for creating Cu matrix composites. Under various wear conditions, the fretting wear behavior of Cu-matrix composites is investigated [16].

Therefore, in this study, the additions of (1–4.5) wt% of micro-size TiC and (0.25–1) wt% for nano-size TiC to Cu powder were done to fabricate samples with cold press consolidation, followed by sintering. The effect of the TiC content on the microstructure, optical properties, hardness, and compression strength of the composites were investigated.

MATERIALS AND METHODS

Cu (99.9 purity) and TiC (99.9 purity) for both nano and micro size, powders were used as starting materials. It was supplied by China Jingan Chemicals and Alloy Limited Company. Table 1 shows the chemical composition of as-received Cu powder.

The combinations of Cu powder and micro size TiC powder with three different content included (1.5, 3 and 4.5) wt% were placed into a 304SS container with 11 diameter mm 1:10 weight ratio of chromium iron balls Each charge was milled at 170 rpm for 7 hours. The milled powders, after being taken out of the ball mill, were pressed to disc-like samples with a diameter of 15 mm. Vickers microhardness (HV) of the balls was measured in mechanical engineering college-Tikrit university using a Metkon microhardness tester with a 500gm applied stress. For the pressing

Table 1. Copper's chemical composition

Powder	Purity%	Average particle size (μm)							
Cu	99.9	150							
Chemical composition wt%									
Cu	Ni	Fe	Mg	C	S	Ca	Na	O	Others
99.8	0.001	0.003	0.001	0.008	0.002	0.001	0.001	0.1	Rem.

step, a uniaxial hydraulic press type KWP 80 M / Germany was employed, with the best selected applied pressing pressure of 700 MPa. The green density of the fabricated samples was estimated using equation (1) [17]. Each sample mass was determined using an electronic balance model OHAUS-USA with a 0.1mg precision. The volume of the samples was computed using the measured major dimensions.

$\rho G = MG / VG$ (1)

ρG: Green compact density (g/cm^3)

MG: Compacted samples mass (gm)

VG: Compacted samples volume (cm^3)

Theoretical density (ρt) and total porosities (Pto) for green compacts (GC) are calculated using the formulae (2 and 3)[18].

$\rho_o = \rho Cu \times wCu + \rho TiC \times wTiC$ (2)

ρt: Theoretical density (g/cm^3).

ρCu, ρTiC: Theoretical density of (Cu, TiC) (g/cm^3) respectively.

wCu, wTiC: %wt of (Cu, TiC) respectively.

GC total porosity was calculated according to equation 3 below:

$PO\% = (1-\rho G / \rho t) \times 100$ (3)

PO: GC total porosity%.

According to the results of (ρG), the best-applied pressure was 700 MPa, hence it was used afterward in the preparation of all GC. The GC are then sintered in an electric resistance furnace type CARBOLITE/UK in an incessantly applied argon gas stream from the start of the sintering to room temperature.

The heating rate is set to 10 degrees Celsius per minute. The samples were held at 850 °C for two hours then the furnace was turned off, and the samples were left to cool slowly within the furnace. The cylindrical samples' parallel faces were wet ground using silicon carbide emery sheets of (500, 1000, 2000, and 3000) grit, and then polished with a 2µm alumina suspension solution, rinsed with distilled water, and ethanol alcohol. The Vickers micro-hardness of the sintered compact samples was determined by Metkon tester with 500 gm applied load. After etching it with a solution consisted of potassium permanganate 4g per 1000 cm3 water and 10-part H2SO4 for 30 sec then washed with distilled water. Optical microscopy using microscope type OPTIKA/Italy was performed. FESEM-EDS and Mapping using ZELSS instrument was utilized for microstructure observation and analysis. X-ray diffraction analysis (XRD) was performed for the used powders and prepared Cu -TiC composites by Shimadzu XRD-6000 Shimadzu-USA using Cu Kα (λ=0.154059 nm)

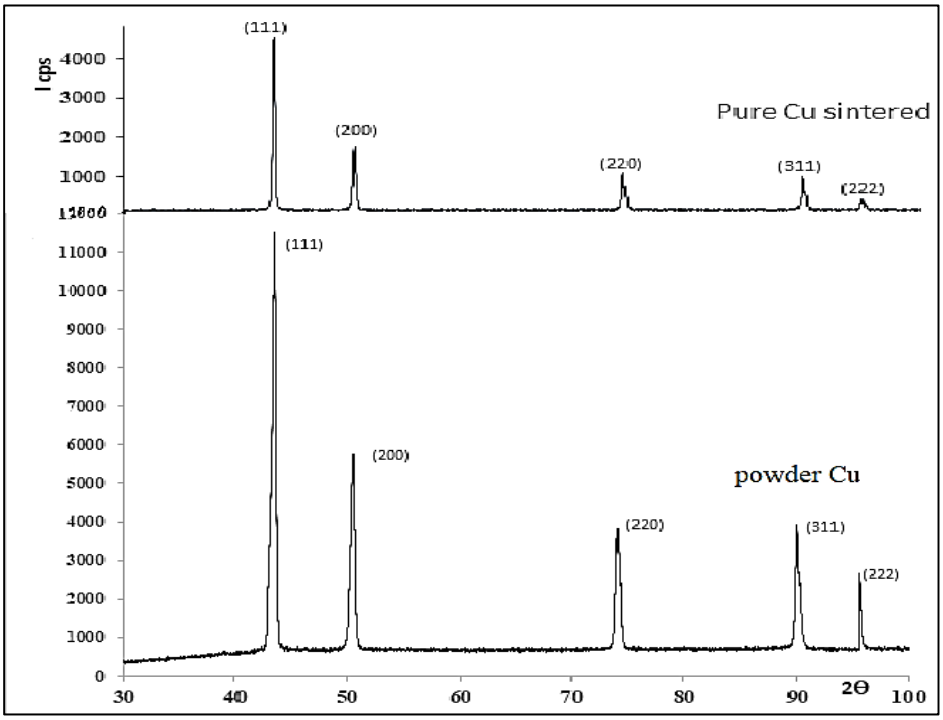

Fig. 1. XRD patterns for Cu powder and sintered compact Cu sample.

radiation with 2θ in the range (30- 100) º.

RESULTS AND DISCUSSION

X-ray diffraction analysis

The X-ray analysis was performed for pure Cu powder, pure Cu sintered compact, and each fabricated Cu-TiC composite type. The phases that form the structure of pure Cu sintered compact ensured the success of the sintering process by means of the observation of the no other phases formed such as copper oxides. This is really clear from the X-ray graphs of the Cu powder and Cu sintered compacted samples shown in Fig. 1 are identical to the standard diffraction peaks of Cu (JCPDS, file No. 04-0836). The only difference that was detected in the intensity of the characteristic peaks of the Cu powder was greater than the corresponded peaks of that are belong to the sintered compacted Cu sample. XRD charts for micro and nano-size TiC powders explained in Fig. 2 that were used in the present study were matched with (JCPDS, file No. 03-065-8417) and the intensity of peaks of micro-size TiC powder was greater than their corresponded ones for nano size TiC powder. It seems from the Fig. 3 and Fig. 4 that depict the XRD charts for the

prepared Cu-TiC composites by several micro and nano TiC additions, respectively, that there is no hint to other phases formation except those referred to the α-Cu phase peaks which were also referred to it in the Fig. 1. It was clear from XRD charts for Cu-TiC composites that the amount of the TiC additions in both micro and nano types were very small in their amount that cannot be revealed by XRD analysis directly. But it is important to observe that the TiC additions made the α-Cu peaks to appear with lower intensity and the intensity of each peak was decreased by increasing the micro or nano-TiC additions. This situation of the XRD graph also demonstrated that there was no chemical reaction between Cu and TiC. XRD graphs obviously show that no oxide phase formed in Cu-TiC composites such as CuO [19,20].The decrease in the intensity with an increase in the content of TiC indicates that the level of arrangement of the atoms decreases in the composite and becomes somewhat less crystalline, this is what was seen from the Fig. 3. But from the observation of Fig. 4 the effect of the nano TiC addition on the value of the Cu peaks intensity was lower than addition of micro size TiC. The reason is mainly due to the lower produced localized strain energy.

Microstructure

The optical micrographs of Cu-TiC composites with various wt% of micro-size TiC particles are illustrated in Fig. 5. The figure explains How the

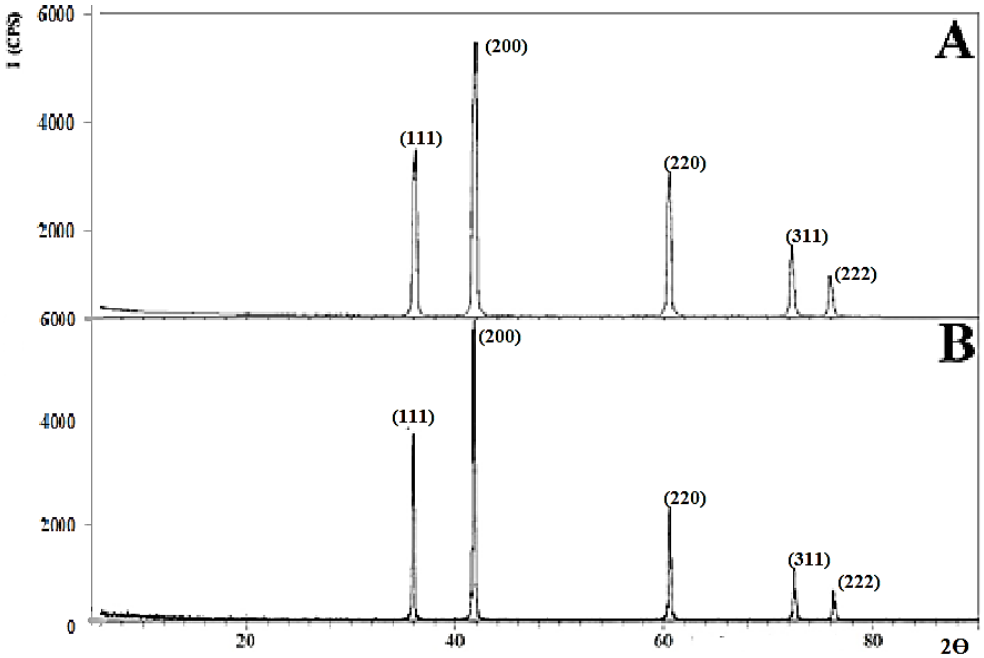

Fig. 2. XRD patterns for TiC powder, A: Nano size and B: Micro size.

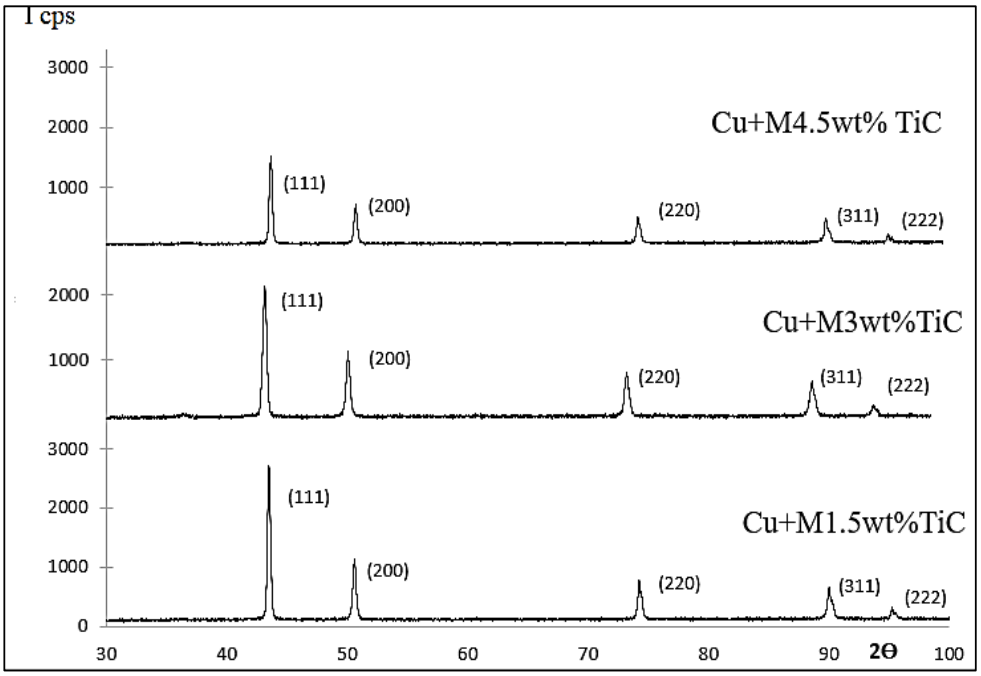

Fig. 3. XRD patterns for sintered compact Cu samples with different micro size TiC addition.

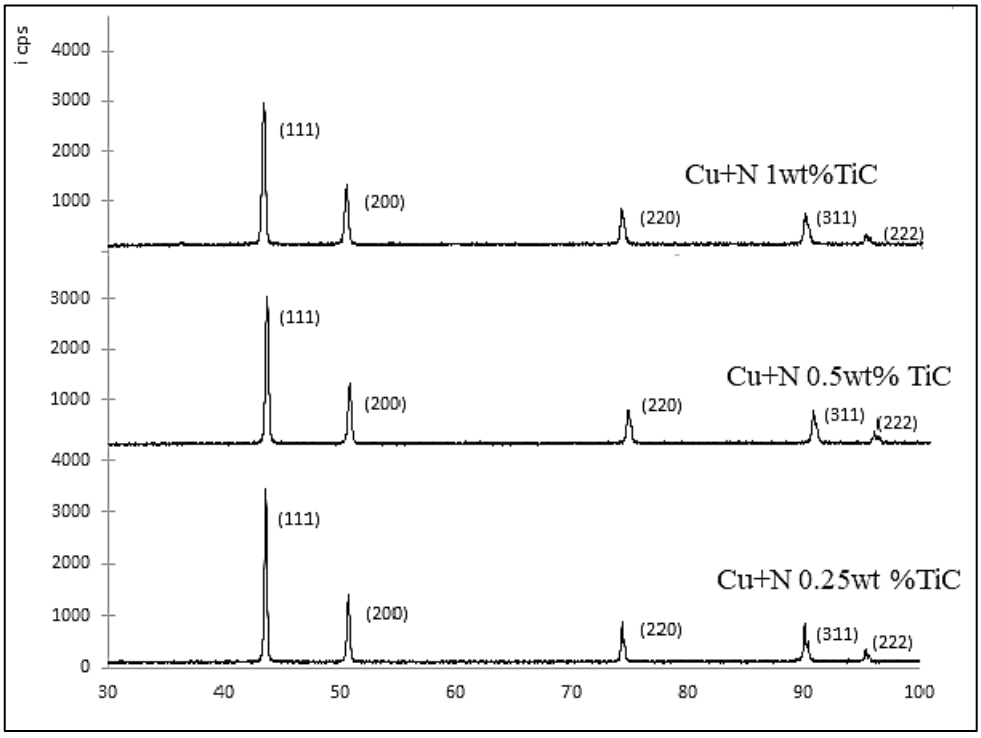

Fig. 4. XRD patterns for sintered compact Cu samples with different nano size TiC addition.

TiC particles distributed between Cu-particles and their area fraction was increased in the observed surface area by optical microscope by the increasing of the TiC wt%. The enlarged image E for a small area of Fig. 5-D shows the interface between the Cu and TiC particles which was free of cracks and

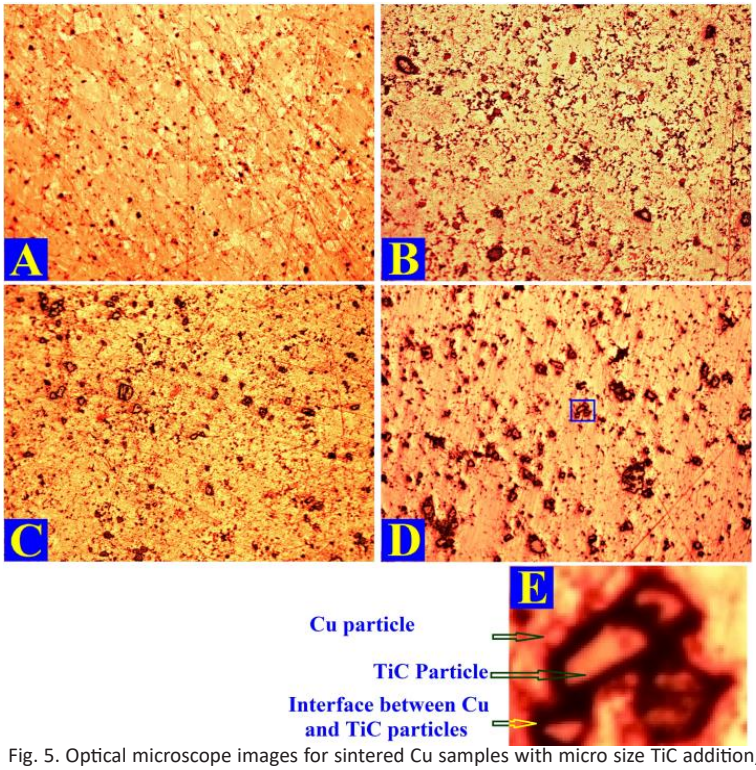

Fig. 5. Optical microscope images for sintered Cu samples with micro size TiC addition, A: 0 wt%, B: 1.5 wt%. C: 3wt% and D: 4.5 wt%. Magnification power 100 X.

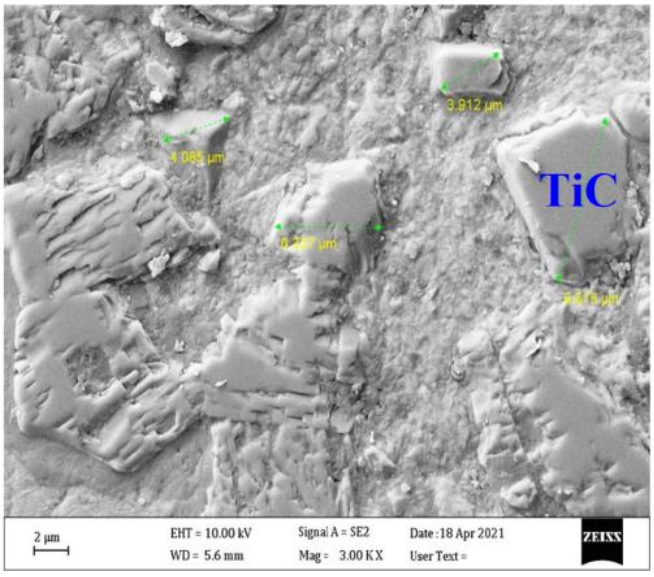

Fig. 6. FESEM image for sintered Cu - TiC with 4.5 wt% micro size TiC addition.

porosity. This situation is more clearly displayed in the observed area from the Cu-TiC composite picked up by FESEM instrument as shown in Fig. 6 where TiC particles are well embedded among Cu particles with no cracks voids or porosities at interface positions between the two different particles. While Fig. 7 explains the presence of the microstructure its two main components and how small size TiC particles that resulted from the breakage of the TiC particle during ball milling

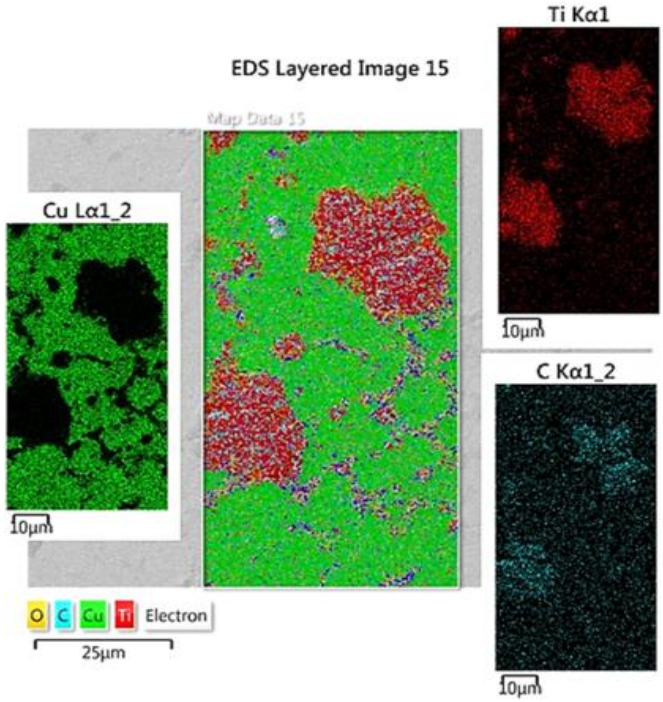

Fig. 7. FESEM - mappingimage for sintered Cu - TiC with4.5 wt% micro size TiC addition.

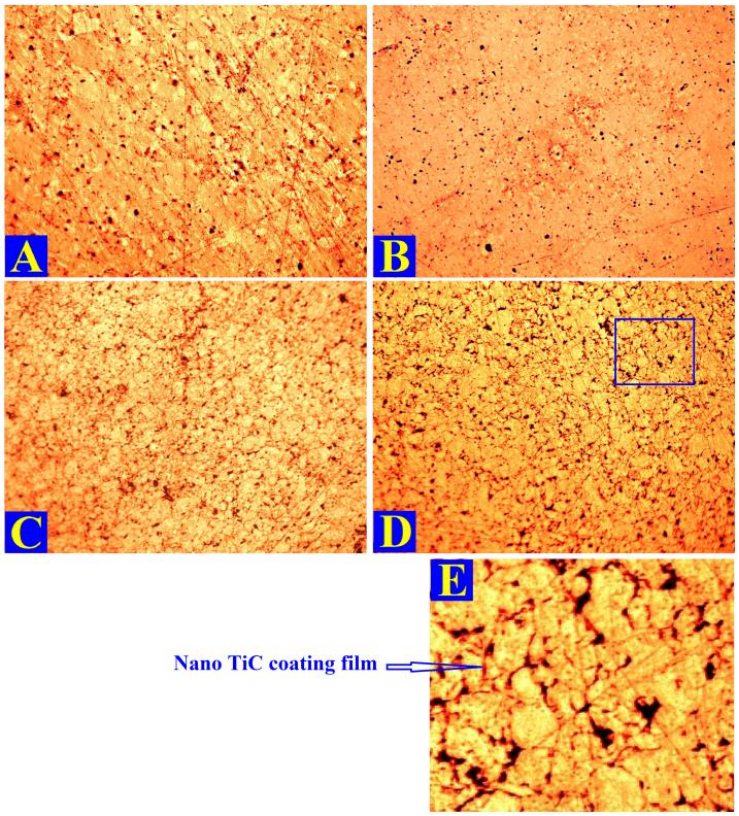

Fig. 8. Optical microscope images for sintered Cu samples with nano size TiC addition, A: 0 wt%, B: 0.25 wt%. C: 0.5 wt% and D: 1 wt%. Magnification power 100 X.

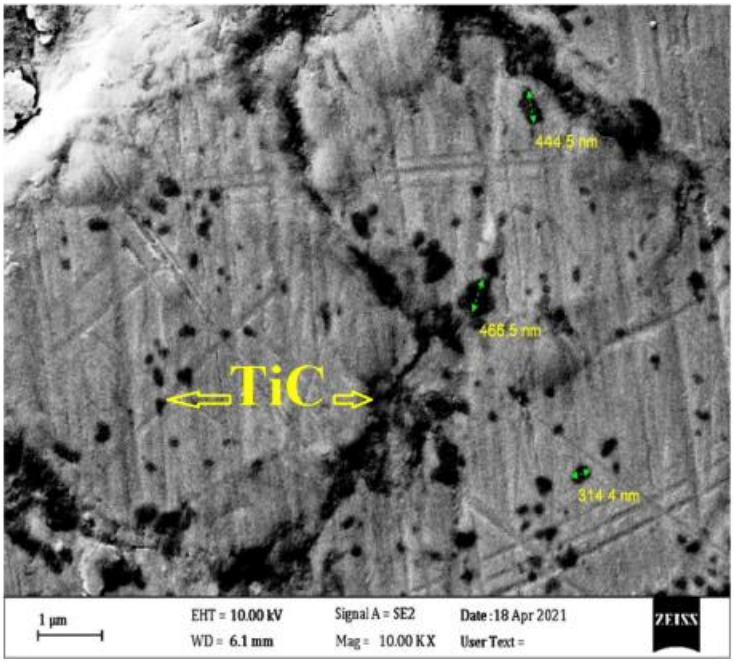

Fig. 9. FESEM image for sintered Cu - TiC with1wt% nano size TiC addition.

and pressing process are distributed between Cu particles.

The optical micrographs of Cu-TiC composites with various wt% of nano-size TiC particles are illustrated in Fig. 8. The optical microscopy indeed does not clarifies exactly how the TiC particles are distributed between Cu-particles. Nevertheless, the approximately large amount addition of nano TiC particle which was 1 wt% made some variation in the microstructure particularly at Cu particles

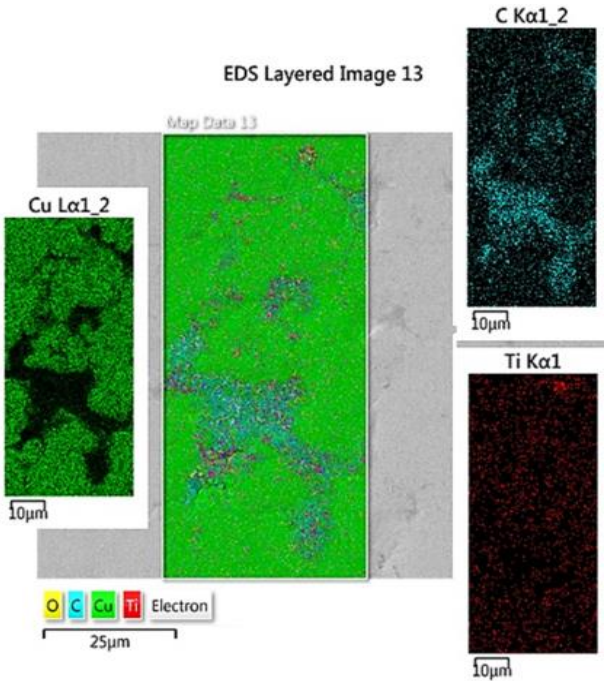

Fig. 10. FESEM - mappingimage for sintered Cu - TiC with1 wt% nano size TiC addition.

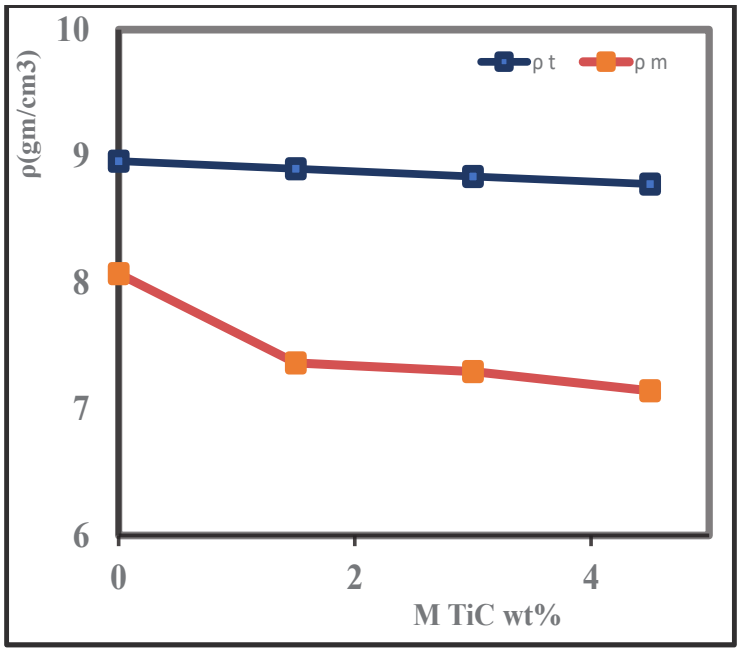

Fig. 11. Theoretical and measured densities for sintered Cu - micro size TiC composites.

boundaries where TiC particles are formed a thin film between Cu particles in lots of positions while the cluster-like shape of several TiC nanoparticles are formed at

some other positions. This situation is more clearly explained in the enlarged image shown in Fig. 8-E.

This distribution of the nano TiC particle is well detected by higher magnification power by the usage of FESEM facility as shown in Fig. 9 where TiC particles with black color are well imbedded within and amongst Cu particles as an interface.

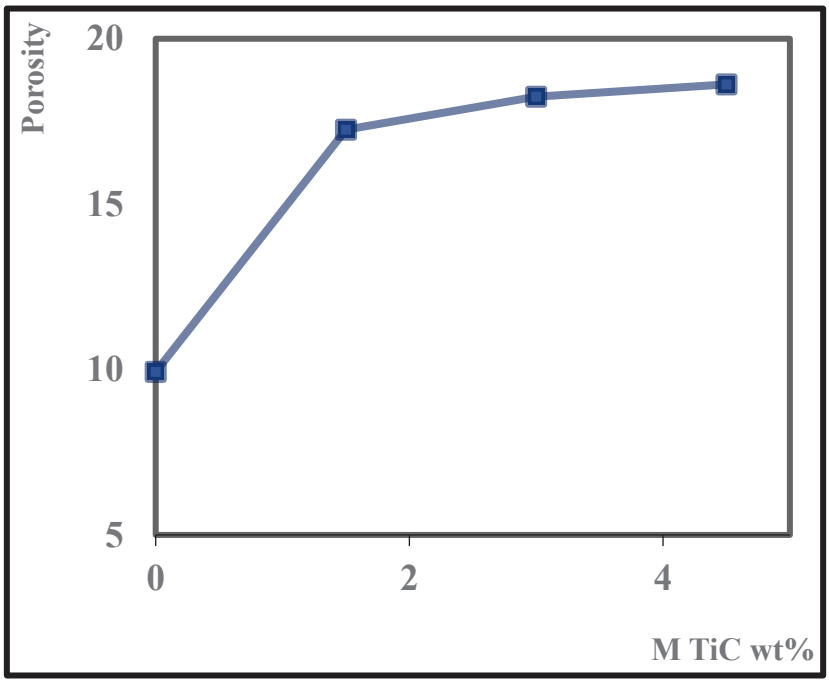

Fig. 12. Porosity variation trend for sintered Cu - micro size TiC composites.

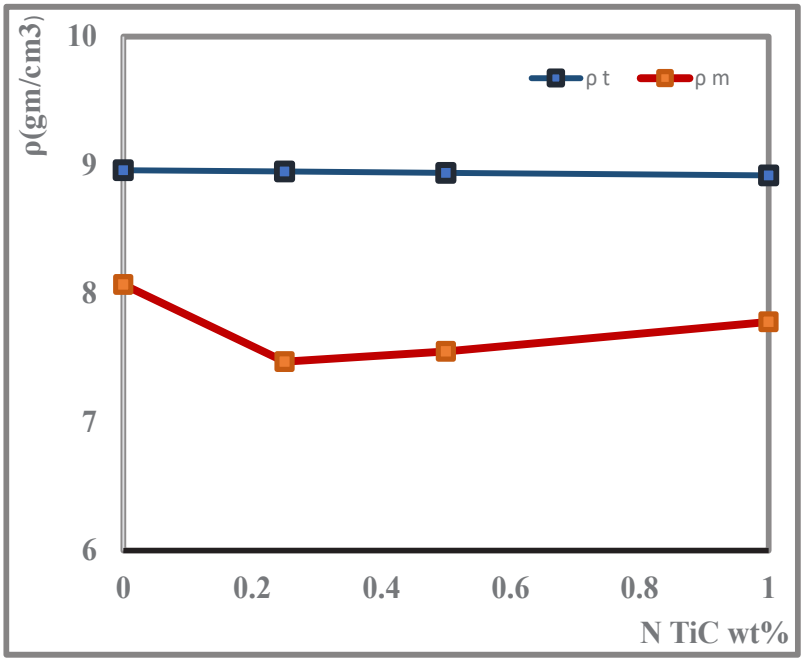

Fig. 13. Theoretical and measured densities for sintered Cu - nano size TiC composites.

In turn Fig. 10 explains the presence of the microstructure its two main particles components and how nano-sized TiC particles were distributed at Cu particles boundaries also within the Cu particles where hard TiC ceramic particles are able to pin inside less hardness Cu particles during ball milling and pressing process as explained in Fig. 9.

Density

The measured density of sintered compacted Cu is lower than its theoretical density as shown in Fig. 11 this is because the mechanically milled Cu has increasing in lattice defects like dislocations and work hardening of milled powders [21]. Densities of the composites were determined and indicated

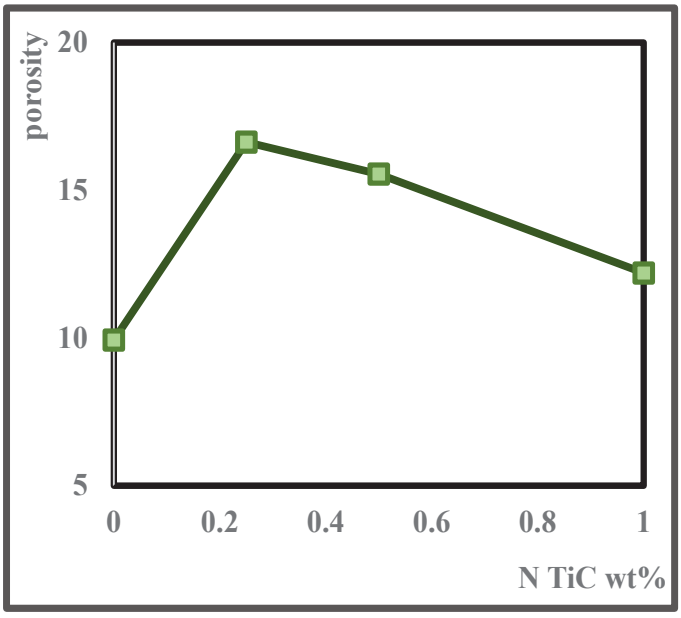

Fig. 14. Porosity variation trend for sintered Cu - nano size TiC

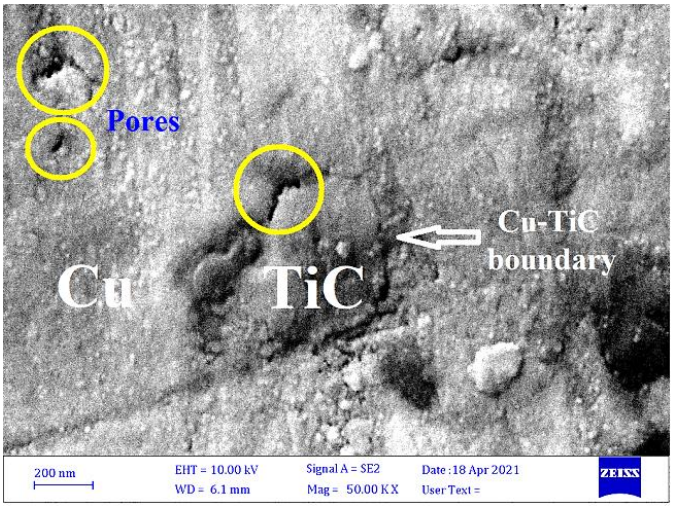

Fig. 15. FESEM image for sintered Cu - TiC with 1wt% nano size TiC addition.

that with increasing TiC addition, their densities decreased because the density of TiC is lower than that of Cu. This effect is actually observed by the calculation of the theoretical density of the Cu- micro size TiC composite which is showed in Fig. 11. Another reason is that with increasing TiC addition the porosity was increased because of the trapped air between TiC particles and Cu-matrix particles, this is because no diffusion will occur between the two different types of particles. Then the effect of TiC addition on both measured density of sintered compacted Cu samples and their porosities are well illustrated in Fig. 11 and Fig. 12 respectively. Accordingly, the minimizing of the pore's size and the amount will depend mainly on the pressing pressure value.

On other hand, the addition of the nano-sized TiC particles does not have any effect on the theoretical density of the Cu because of its low amounts addition. But the measured density of the sintered compacted samples was decreased by 0.25 wt% addition of TiC as shown in Fig. 13,

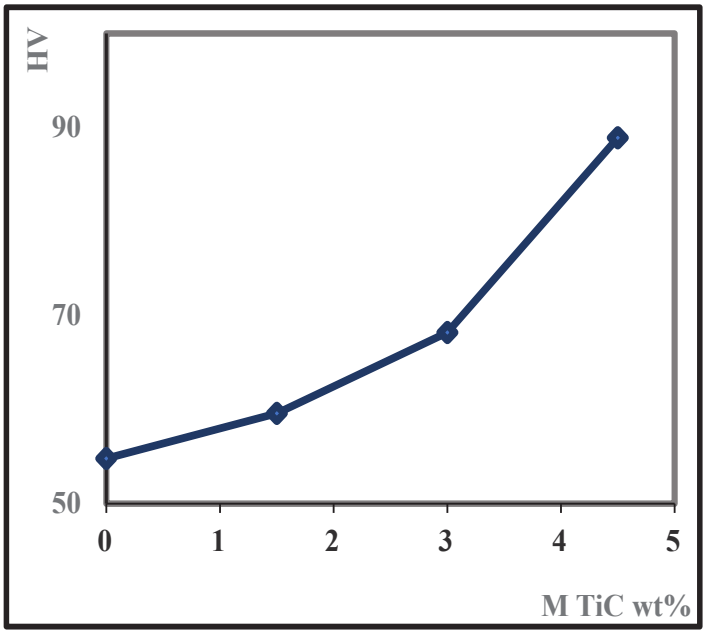

Fig. 16. Micro hardness variation for sintered Cu - micro size TiC composites.

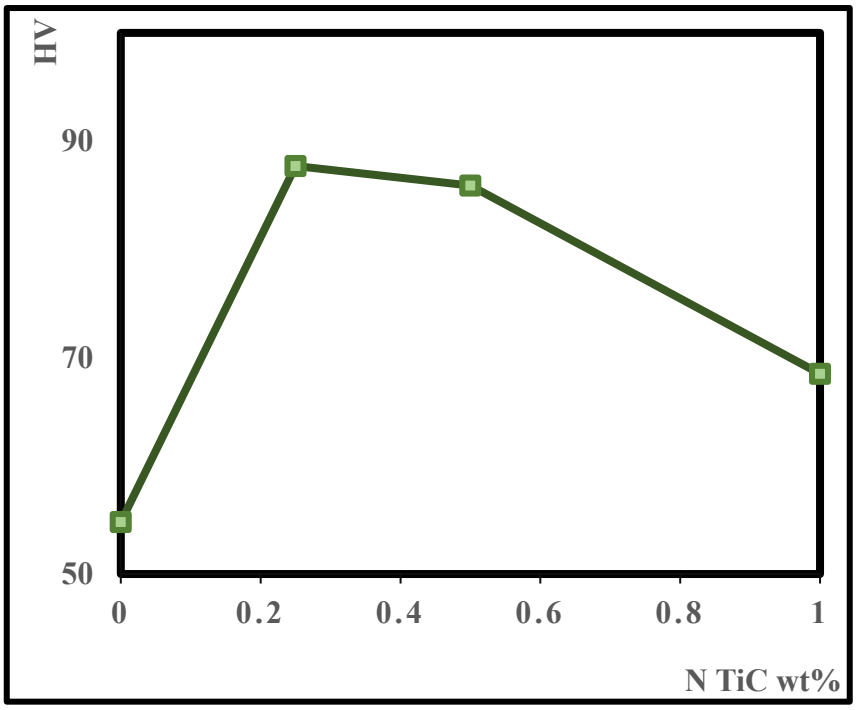

Fig. 17. Micro hardness variation for sintered Cu - bano size TiC composites.

then it was continually increased by increasing the nanoparticle addition, but it remained with lower values than the density of the sintered compact samples of pure Cu. This trend of the measured

density change is reflected in the values of the calculated porosity of the Cu- nano TiC composites as illustrated in Fig. 14. The most important observation was that the addition of nano-sized TiC particles with values greater than 0.25 wt% tends to occupy the remained pores between the Cu particles during the pressing step which is well reflected in the decrease of the porosity value and increase of the density of the sintered sample.

The formed pores in the sintered Cu- nano TiC composites were mainly existed at the interface zone between Cu and TiC particles as shown in Fig. 15, where the pores have irregular shapes as is explained in the areas denoted by yellow circles.

Hardness

Cu dislocation density was enhanced by adding TiC particles to the mix. During indentation, the interaction between TiC particles and dislocation density increases microhardness. The dislocation density will increase as the volume fraction of TiC particles increases. As a result, with a greater volume percentage of TiC particles, the contact will be stronger, improving hardness even more. the hardness values of micro TiC - Cu composites increased from 54.8 to 88.9 HV with the addition of 4.5 wt % TiC as illustrated in Fig. 16. The immediate presence of hard ceramic particulates in a soft metallic matrix leads to an improvement in the hardness. The resistance to the transferred load from the Cu matrix to the TiC reinforcement is expected to be more because of the higher strength and hardness of the ceramic particles than the softer Cu matrix which may be another reason for higher hardness. When Cu powder was mixed with nano TiC particles in three weight fractions (0.25, 0.5, and 1) %. The hardness of the fabricated composite was improved as compared with pure Cu, where it reached the maximum value at 0.25 wt% TiC, then it decreased but its value remained higher than that for pure Cu sintered compacts, as shown in Fig. 17. The thought is due to the wider spread of the agglomerated nano TiC between Cu particles above the critical concentration (0.25 wt%) of the nano addition. Another factor that could have to participate to enhance the hardness initially is the effective “dispersion strengthening” by the introduction of nano TiC granules to the Cu matrix [22,23].

CONCLUSION

1. The prepared pure Cu and its composites

with micro and nano-size TiC additions were free of oxidization which was detected from XRD analysis.

2. The results revealed that as the micro and nano TiC content increases, the density of the sintered copper decreases.

3. Generally the micro sizes TiC additions tend to increase the porosity of sintered copper samples, while the increase of the porosity was in lower values particularly when the nano TiC addition was greater than 0.25 wt%.

4. The increase in micro TiC addition is reflected in the increase of the micro-hardness of sintered copper, while the best micro-hardness value was measured for the sintered copper sample with the lowest nano TiC addition that was 0.25 wt%.

5. The FESEM technique revealed that the micro size TiC particles were strongly embedded in the Cu matrix. On other hand, the nano-size TiC particles are well distributed amongst Cu powder particles and with them.

CONFLICT OF INTEREST

The authors declare that there are no conflicts of interest regarding the publication of this manuscript.

REFERENCES

1. Singh L. Latest Developments in Composite Materials. IOSR Journal of Engineering. 2012;02(08):152-158.
2. Ding H, Chu W, Liu Q, Wang H, Hao C, Jia H, et al. Microstructure evolution of Cu-TiC composites with the change of Ti/C ratio. Results in Physics. 2019;14:102369.
3. Kargul M, Borowiecka-Jamrozek J, Konieczny M. The effect of reinforcement particle size on the properties of Cu-Al2O3 composites. IOP Conference Series: Materials Science and Engineering. 2018;461:012035.
4. He X, Zou G, Xu Y, Zhu H, Jiang H, Jiang X, et al. Nano-mechanical and tribological properties of copper matrix composites reinforced by graphene nanosheets. Progress in Natural Science: Materials International. 2018;28(4):416-421.
5. Song W-w. Electrochemical Corrosion Performance of FSSP-Modified Copper Alloy Surface. International Journal of Electrochemical Science. 2019:7026-7036.
6. Ouml, zg, uuml, n, Ouml, zg, et al. Powder Metallurgy Mg-Sn alloys: Production and characterization. Sci Iranica. 2019;0(0):0-0.
7. Hu Z-J, Shen P, Jiang Q-C. Developing high-performance laminated Cu/TiC composites through melt infiltration of Ni-doped freeze-cast preforms. Ceram Int. 2019;45(9):11686-11693.
8. Zhang D, Liu H, Sun L, Bai F, Wang Y, Wang J. Shape-Controlled TiCx Particles Fabricated by Combustion Synthesis in the Cu-Ti-C System. Crystals. 2017;7(7):205.
9. Nguyen Thi Hoang O, Nguyen Hoang V, Kim J-S, Dudina D. Structural Investigations of TiC–Cu Nanocomposites Prepared by Ball Milling and Spark Plasma Sintering. Metals. 2017;7(4):123.
10. Xu X, Li W, Wang Y, Dong G, Jing S, Wang Q, et al. Study of the preparation of Cu-TiC composites by reaction of soluble Ti and ball-milled carbon coating TiC. Results in Physics. 2018;9:486-492.
11. Ding H, Liu Q, Wang X, Fan X, Krzystyniak M, Glandut N, et al. Effects of boron addition on the microstructure and properties of in situ synthesis TiC reinforced Cu Ti C composites. J Alloys Compd. 2018;766:66-73.
12. Rathod S, Modi OP, Prasad BK, Chrysanthou A, Vallauri D, Deshmukh VP, et al. Cast in situ Cu–TiC composites: Synthesis by SHS route and characterization. Materials Science and Engineering: A. 2009;502(1-2):91-98.
13. Dong, Qiu, Li, Shu, Yang, Jiang. The Synthesis, Structure, Morphology Characterizations and Evolution Mechanisms of Nanosized Titanium Carbides and Their Further Applications. Nanomaterials. 2019;9(8):1152.
14. Bohórquez CD, Pérez S, Sarmiento A, Mendoza M. Sintering of a metal matrix composite Cu-Ti-TiC assisted by abnormal glow discharge. Journal of Physics: Conference Series. 2019;1386(1):012043.
15. Jie Y, Jiang KY. Multi-Response Optimization of TiC-Cu P/M Composite Physical Properties. Advanced Materials Research. 2013;788:73-76.
16. Akhtar F, Askari SJ, Shah KA, Du X, Guo S. Microstructure, mechanical properties, electrical conductivity and wear behavior of high volume TiC reinforced Cu-matrix composites. Mater Charact. 2009;60(4):327-336.
17. Yagoob JA, Abbass MK. Characterization of Cobalt Based CoCrMo Alloy Fabricated by Powder Metallurgy Route. 2018 2nd International Conference for Engineering, Technology and Sciences of Al-Kitab (ICETS); 2018/12: IEEE; 2018.
18. Mahdi FM, Eaqoob JA, Muhialdeen FR. Mechanical and Physical Properties of Hybrid Cu-Graphite Composites Prepared via Powder Metallurgy Technique. Tikrit Journal of Engineering Sciences. 2017;24(1):11-24.
19. Dang KQ, Nguyen YN, Hoang QA, Tran HV, Nguyen MC, Pham HV, et al. DENSIFICATION AND MECHANICAL PROPERTIES OF FEMN13-TiC COMPOSITES FABRICATED BY PULSED ELECTRIC CURRENT SINTERING PROCESS. Acta Metallurgica Slovaca. 2018;24(4):273-279.
20. Buytoz S, Dagdelen F, Islak S, Kok M, Kir D, Ercan E. Effect of the TiC content on microstructure and thermal properties of Cu–TiC composites prepared by powder metallurgy. J Therm Anal Calorim. 2014;117(3):1277-1283.
21. Bagheri GA. The effect of reinforcement percentages on properties of copper matrix composites reinforced with TiC particles. J Alloys Compd. 2016;676:120-126.
22. Hussein MK, Jameel WW, Sabah NFA. Fabrication of Copper-Graphite MMCs Using Powder Metallurgy Technique. Journal of Engineering. 2018;24(10):49-59.
23. Safardoust-Hojaghan H, Amiri O, Salavati-Niasari M, Hassanpour M, Khojasteh H, Foong LK. Performance improvement of dye sensitized solar cells based on cadmium sulfide/S, N co doped carbon dots nanocomposites. J Mol Liq. 2020;301:112413.